Neutrino decoherence and the mass hierarchy in the JUNO experiment

E. Marzec and J. Spitz
University of Michigan, Ann Arbor, Michigan 48109, USA

(Received 18 August 2022; accepted 16 September 2022; published 28 September 2022)

The finite size of a neutrino wave packet at creation can affect its oscillation probability. Here, we consider the electron antineutrino wave packet and decoherence in the context of the nuclear reactor-based experiment JUNO. Given JUNO's high expected statistics [~100k IBD events ($\bar{\nu}_e p \to e^+ n$)], long baseline (~53 km), and excellent energy resolution [$\sim 0.03/\sqrt{E_{\rm vis}(\rm MeV)}$], its sensitivity to the size of the wave packet is expected to be quite strong. Unfortunately, this sensitivity may weaken the experiment's ability to measure the orientation of the neutrino mass hierarchy for currently allowed values of the wave-packet size. Here, we report both the JUNO experiment's ability to determine the hierarchy orientation in the presence of a finite wave packet and its simultaneous sensitivity to size of the wave packet and the hierarchy. We find that wave-packet effects are relevant for the hierarchy determination up to nearly two orders of magnitude above the current experimental lower limit on the size, noting that there is no theoretical consensus on the expectation of this value. We also consider the effect in the context of other aspects of JUNO's nominal three-neutrino oscillation measurement physics program and the prospect of future enhancements to sensitivity, including from precise measurements of Δm^2_{3l} and a near detector.

DOI: 10.1103/PhysRevD.106.053007

I. INTRODUCTION

The plane-wave treatment of neutrino oscillations, in which the propagating neutrino is assigned a definitive momentum, is an excellent approximation for terrestial- and atmospheric-based neutrino experiments. This framework breaks down, however, in the case that the neutrino wave packet is finite (see, e.g., Refs. [1–5]). The different velocities of the propagating mass eigenstates lead to their separation and change the oscillation probability, with the effect increasing for larger travel distances, lower energies, and larger mass splittings. All observed neutrino oscillation signatures, with the possible exception of solar and supernova neutrinos which are expected to be completely decoherent, are so far consistent with coherent neutrino oscillations due to the relatively small size of the observable contributions compared to experimental resolutions. However, the increasing capability of neutrino experiments makes gaining sensitivity to the finite size of the wave packet a reasonable future possibility.

Originating inside of a nuclear reactor and with contributions from the beta decays of some ~1000 isotopes [6], the typical size of an electron antineutrino wave packet at creation, denoted by σ_x, is at present unknown. However, there is potential for performing this detailed and complex calculation in the future, *à la* Ref. [7]. For now, the distance scales of the decay, including the characteristic beta-decay-nucleus size ($\sim 10^{-5}$ nm) and the inverse of the antineutrino energy ($\sim 10^{-4}$ nm) [8], considered alongside the current reactor-based limits ($\sigma_x > 2.1 \times 10^{-4}$ nm at 90% C.L. using a phenomenological combination of Daya Bay, KamLAND, and RENO data [8], and $\sigma_x > 1 \times 10^{-4}$ nm at 95% C.L. from a dedicated measurement with Daya Bay [9]), motivate a study of the effects of σ_x on experimental observables for values as low as 10^{-4} nm. We note, however, that the other relevant distance scale in the decay, the interatomic spacing of the uranium-based fuel (~0.1–1 nm), is well above the level at which wave-packet effects would be discernible in any realistic future reactor-based experiment.

Expecting first data in 2023, the ambitious JUNO project is at the forefront of what is possible with a reactor antineutrino experiment [10,11]. The experiment will feature a 20-kton liquid scintillator far detector about 53 km from a 26.6-GWth total set of pressurized water reactor (PWR) complexes. With 77.9% photocoverage, JUNO can expect $\sim 0.03/\sqrt{E_{\rm vis}(\rm MeV)}$ positron visible energy resolution for characterizing the ~100k IBD events ($\bar{\nu}_e p \to e^+ n$) expected in the data collection period (6 yr). As has been shown in Refs. [12,13], the high statistics, long baseline, and strong energy resolution of JUNO translate to more than an order of magnitude better sensitivity to the wave-packet effect as compared to previous reactor experiments, including Daya Bay [14], KamLAND [15], and RENO [16].

The effect of a finite wave-packet size on the oscillation probability is easy to demonstrate by considering atmospheric-only electron-flavor disappearance (with normal mass ordering):

$$P_{ee} \to 1 - \frac{1}{2}\sin^2 2\theta_{13} \times \left[1 - \cos\frac{1.27\Delta m^2_{31} L}{E} \exp\left(-\frac{L^2(\Delta m^2_{31})^2}{32E^4\sigma_x^2}\right)\right]. \quad (1)$$

We see that the dampening of the oscillation probability due to the wave-packet size (σ_x) increases with L, decreases with E, and increases with Δm^2. As such, the effect is larger for sterile ($\Delta m^2 \sim 1$ eV^2) [17] and atmospheric oscillations ($\Delta m^2 \sim 3 \times 10^{-3}$ eV^2) as compared to solar oscillations ($\Delta m^2 \sim 7 \times 10^{-5}$ eV^2). JUNO's large L (~53 km), low $E_{\bar{\nu}_e}$ (~2–10 MeV), and sensitivity to the atmospheric mass splitting makes it an excellent testing ground for the effect of σ_x on oscillation behavior. In general, one can expect JUNO to be more sensitive to wave-packet effects within the three-neutrino oscillation paradigm [17], at least, than any existing or even near-term-planned experiment.

In addition to the wave-packet effect, JUNO's extraordinary capability also makes it sensitive to the orientation of the neutrino mass hierarchy, among other oscillation parameters [10,11]. The three-neutrino oscillation probability in vacuum and without the wave-packet effect is given by $P_{ee} = 1 - P_{21} - P_{31} - P_{32}$, with

$$P_{21} = \cos^4\theta_{13}\sin^2 2\theta_{12}\sin^2\left(\frac{1.27\Delta m^2_{21} L}{E}\right)$$
$$P_{31} = \cos^2\theta_{12}\sin^2 2\theta_{13}\sin^2\left(\frac{1.27\Delta m^2_{31} L}{E}\right)$$
$$P_{32} = \sin^2\theta_{12}\sin^2 2\theta_{13}\sin^2\left(\frac{1.27\Delta m^2_{32} L}{E}\right). \quad (2)$$

The difference in oscillation probability between the normal hierarchy ($m_3 > m_2 > m_1$) and inverted hierarchy ($m_2 > m_1 > m_3$) for the JUNO experiment can be seen in Fig. 1 in terms of IBD-based reconstructed antineutrino energy ($E_{\bar{\nu}_e} = E_{e^+} + 0.78$ MeV), with and without energy resolution smearing according to the expected positron energy resolution (see below).

The discernible shape difference between the hierarchies is reduced with oscillation dampening due to a finite wave-packet size. The three-neutrino oscillation equation [Eq. (2)] is modified to include wave-packet effects with

$$P_{21} = \cos^4\theta_{13}\sin^2 2\theta_{12}\cdot\frac{1}{2}\left[1 - \cos\frac{1.27\Delta m^2_{21} L}{E}\cdot \exp\left(-\frac{L^2(\Delta m^2_{21})^2}{32E^4\sigma_x^2}\right)\right]$$
$$P_{31} = \cos^2\theta_{12}\sin^2 2\theta_{13}\cdot\frac{1}{2}\left[1 - \cos\frac{1.27\Delta m^2_{31} L}{E}\cdot \exp\left(-\frac{L^2(\Delta m^2_{31})^2}{32E^4\sigma_x^2}\right)\right]$$
$$P_{32} = \sin^2\theta_{12}\sin^2 2\theta_{13}\cdot\frac{1}{2}\left[1 - \cos\frac{1.27\Delta m^2_{32} L}{E}\cdot \exp\left(-\frac{L^2(\Delta m^2_{32})^2}{32E^4\sigma_x^2}\right)\right]. \quad (3)$$

Figure 1 shows the dampening effect of $\sigma_x = 10^{-12}$ m, for example, on the oscillation probability in the case of a normal hierarchy. As can be seen, the fast-atmospheric oscillation probability, with frequency governed by Δm^2_{3l} [18], is washed out and the power to distinguish the hierarchies is significantly reduced, especially at lower antineutrino energies where the effect is more pronounced. Fortunately, however, while the amplitude of oscillation

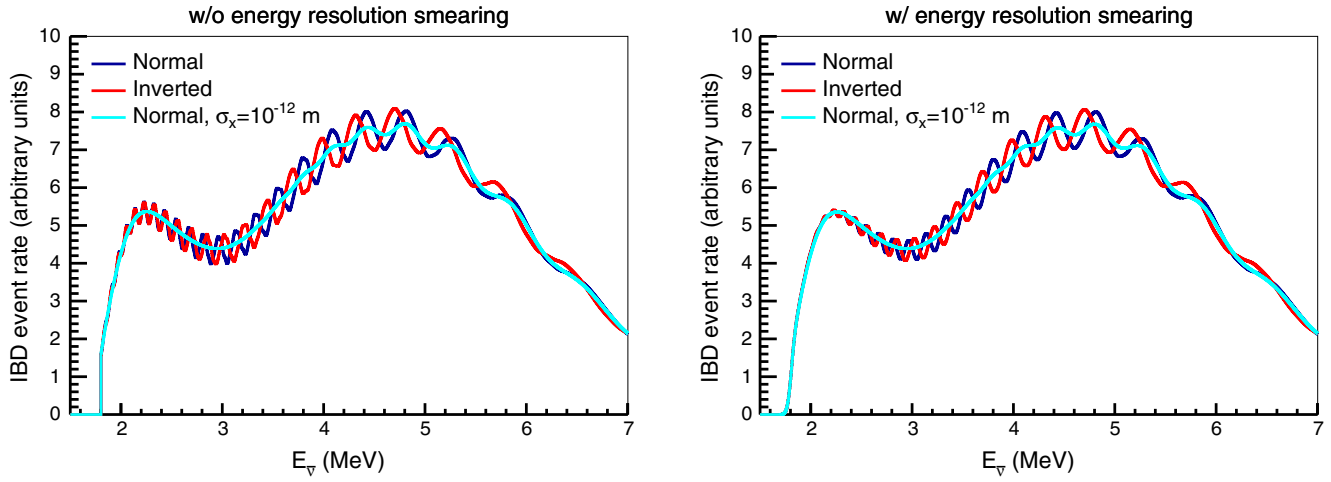

FIG. 1. The IBD event rate distribution shapes expected at JUNO, without (left) and with (right) energy smearing due to reconstruction resolution. The shape differences between the normal and inverted hierarchy are shown. In addition, the dampening effect of finite σ_x (10^{-12} m) on the normal hierarchy oscillation probability can be seen.

decreases, the oscillation frequency and phase is left unchanged by the wave-packet size. Therefore, while the finite size of the wave packet can lead to diminished, or even nullified (in the case that the fast-atmospheric oscillations completely disappear), sensitivity to a hierarchy determination, it is unlikely to lead to a confused or systematically incorrect determination.

Previous work has considered the effect of the wave-packet size on hierarchy determination in generic medium baseline reactor experiments [19], and JUNO's sensitivity to the size of the wave packet with a known hierarchy [12,13]. Below, we report the JUNO experiment's ability to determine the hierarchy in the presence of a finite wave packet, with an emphasis on *experimentally allowed* values of this parameter, again noting that there is no reliable theoretical prediction, and consider JUNO's sensitivity to both the wave-packet size and the orientation of the hierarchy at the same time. The experimental assumptions and analysis methods are detailed in the next section, followed by a section presenting the results and discussion, and then conclusions.

II. ANALYSIS

To model the JUNO experiment, we use the reactor electron antineutrino spectrum as described in Ref. [20] with a PWR fuel mixture consistent with Ref. [10] ($^{235}\mathrm{U}:^{238}\mathrm{U}:^{239}\mathrm{Pu}:^{241}\mathrm{Pu} = 0.577:0.076:0.295:0.052$). Nine relevant PWR nuclear reactor complexes create the antineutrino flux, and their powers and distances from the JUNO detector are modeled according to Ref. [11]. The largest contributions come from the Yangjiang (61.5% of total flux) and Taishan (32.1%) Nuclear Power Plant complexes at around a 53-km baseline. Uncertainties from the reactor flux shape are expected to contribute at the sub-1% level with the inclusion of data from a near detector called "JUNO-TAO" [21]. Construction of JUNO-TAO is ongoing and first data are expected in 2022. The existence of this near detector in constraining the flux-shape uncertainty is implicitly assumed throughout this analysis. At the sub-1% level, the reactor flux-shape uncertainties are not expected to significantly affect either the hierarchy determination or sensitivity to σ_x. Similarly, the reactor flux normalization uncertainty contribution to the sensitivity can be considered negligible [10]. We ignore both sources of flux uncertainty in this analysis.

After creation, the electron antineutrinos are propagated from each reactor, appropriately weighted by distance and power, to the JUNO far detector while applying the three-neutrino oscillation equation, including the different baselines [Eq. (3)]. The central-value three-neutrino oscillation parameters and uncertainties are taken from NuFIT 5.0, including Super-K atmospheric data [22]. Correlations among the parameters are ignored when sampling from the allowed ranges. Also, while terrestrial matter effects provide corrections to $\sin^2\theta_{12}$ and Δm^2_{21} at the 0.5–1.0% level for these distances and energies, they are negligible for $\sin^2\theta_{13}$ and Δm^2_{3l}, and the associated hierarchy and σ_x discussion, and are ignored here for simplicity.

In addition to the standard oscillations, σ_x values from 10^{-13}–10^{-9} m are considered as contributing to the effective oscillation probability. The lower end of this range roughly corresponds to the current experimental limit ($\sigma_x > 2.1\times10^{-4}$ nm at 90% C.L. [8]) and the upper end roughly corresponds to the largest relevant distance scale of the antineutrino-producing beta decay(s), the upper end of the interatomic spacing of the uranium-based fuel. We consider a single σ_x value as affecting the oscillation probability of all $\bar{\nu}_e$ from all reactor complexes considered here noting that a, likely small, range of relevant σ_x values will contribute in reality given the different environmental conditions affecting the size of the wave packet in each reactor core and even individual isotope. For simulating electron antineutrino-induced IBD events, we use the IBD cross section from Ref. [23]. The resulting positron energy spectrum is smeared by the following energy resolution to simulate JUNO's energy reconstruction capability [11]:

$$\frac{\sigma_{E_{\mathrm{vis}}}}{E_{\mathrm{vis}}} = \sqrt{\left(\frac{a}{\sqrt{E_{\mathrm{vis}}}}\right)^2 + b^2 + \left(\frac{c}{E_{\mathrm{vis}}}\right)^2}, \tag{4}$$

with $a = 2.61\%$, $b = 0.82\%$, $c = 1.23\%$ and E_{vis} in MeV. Notably, the nonlinear response of the liquid scintillator due to the "quenching effect" is not accounted for in this resolution estimate. The reader is referred to Refs. [11,24] for more on this relevant issue, which is ignored here for simplicity.

The representative JUNO dataset size is assumed to be 100k electron antineutrino IBD events after standard oscillations [11], from 6 yr of running, and we consider this sample in 200 equally spaced reconstructed antineutrino energy bins from 1.8 to 8 MeV. The statistical and shape uncertainties from all backgrounds (mainly originating from geoneutrinos, fast neutrons, accidentals, and the decays of cosmogenic-induced isotopes) are expected to have a minimal impact on hierarchy sensitivity [10] and are ignored here. A summary of the experimental parameter assumptions is shown in Table I.

With the goal of differentiating one hierarchy from another, we follow Ref. [10] in forming a χ^2 test statistic, comparing the simulated "observed" events (O) in each reconstructed electron antineutrino energy bin (i) to a "prediction" (P) under a particular oscillation+wave-packet scenario:

$$\chi^2 = \sum_{i=1}^{200} \frac{[O_i - P_i(1+\sum_k \alpha_{ik}\epsilon_k)]^2}{P_i} + \sum_k \frac{\epsilon_k^2}{\delta_k^2}. \tag{5}$$

A "fake dataset" observed spectrum (O_i) is created with a particular hierarchy and σ_x value, along with oscillation

TABLE I. Summary of the relevant experimental parameter assumptions.

Experimental parameters	
Total IBD events (~6 yr)	10^5 (post oscillations)
IBD cross-section shape	Vogel and Beacom [23]
e^+ visible energy resolution	See Eq. (4)
Near detector?	Yes, JUNO-TAO [21]
Reactor flux shape	Vogel and Engel [20]
Fuel composition	
^{235}U:^{238}U:^{239}Pu:^{241}Pu	0.577:0.076:0.295:0.052
9 reactor complexes [power (GWth), baseline (km)]	[4.6, 52.77], [4.6, 52.64], [2.9, 52.74], [2.9, 52.82], [2.9, 52.41], [2.9, 52.49], [2.9, 52.11], [2.9, 52.19], [17.4, 215]
Oscillation parameters (3ν)	
θ_{12} (°)	$33.44^{+0.77}_{-0.74}$
θ_{23} (°)	$49.2^{+1.0}_{-1.3}$
θ_{13} (°)	$8.57^{+0.13}_{-0.12}$
Δm^2_{21} (eV^2)	$(7.42^{+0.21}_{-0.20}) \times 10^{-5}$
$\Delta m^2_{31_{\mathrm{NH}}}$ (eV^2)	$(2.515 \pm 0.028) \times 10^{-3}$
$\Delta m^2_{32_{\mathrm{IH}}}$ (eV^2)	$(-2.498^{+0.028}_{-0.029}) \times 10^{-3}$

parameters sampled according to their central values and uncertainties shown in Table I, and the statistics expected in the experiment. The prediction (P_i) is varied to find the χ^2_{min}, while pull terms on the oscillation parameters (ϵ_k, with an α_{ik} fractional contribution to P_i) and associated uncertainties (δ_k) (shown in Table I) are used to constrain the prediction in the minimization procedure, and the σ_x parameter is left unconstrained.

Sensitivity to the mass hierarchy determination can be quantified by comparing the χ^2_{min} with a normal hierarchy-based prediction to the χ^2_{min} with an inverted hierarchy-based prediction:

$$\Delta\chi^2_{\mathrm{MH}} = \chi^2_{\mathrm{min}}(\mathrm{NH}) - \chi^2_{\mathrm{min}}(\mathrm{IH}). \tag{6}$$

$\Delta\chi^2_{\mathrm{MH}}$ will strongly depend on whether the observed spectrum (O_i) was produced with an underlying normal hierarchy or an underlying inverted hierarchy. That is, the sensitivity to hierarchy determination can be dependent on the true underlying hierarchy. We use a subscript on $\Delta\chi^2$ to denote the underlying "true" orientation used to produce the observed sample (i.e., either $\Delta\chi^2_{\mathrm{NH}}$ or $\Delta\chi^2_{\mathrm{IH}}$).

To summarize, we test JUNO's ability to resolve the mass hierarchy for an unknown σ_x by considering many different underlying "true" σ_x values with a known hierarchy. At each scanned true value of σ_x, a JUNO fake dataset "observed spectrum" is produced. A fit is then done to that simulated dataset under both a normal hierarchy hypothesis and an inverted hierarchy hypothesis, with all neutrino mixing parameters allowed to vary as part of the fit according to Table I. In addition, a hypothesized σ_x value is varied as part of the fit. The best-fit χ^2 values for the normal-hierarchy fit and the inverted-hierarchy fit are then compared to produce a $\Delta\chi^2_{\mathrm{MH}}$ for finding the level of statistical separation JUNO will be able to achieve between the two hierarchies. This process is then repeated for each true σ_x value many times to create multiple "universes." The distribution of results across these simulated universes characterizes JUNO's ability to measure the mass hierachy and σ_x accounting for both experimental uncertainty and uncertainty on the mixing parameters.

III. RESULTS AND DISCUSSION

The $\Delta\chi^2_{\mathrm{NH}}$ and $\Delta\chi^2_{\mathrm{IH}}$ distributions of universes are shown with two example σ_x values, 10^{-12} m and 5×10^{-10} m, in Fig. 2. As can be seen, the distinction between the

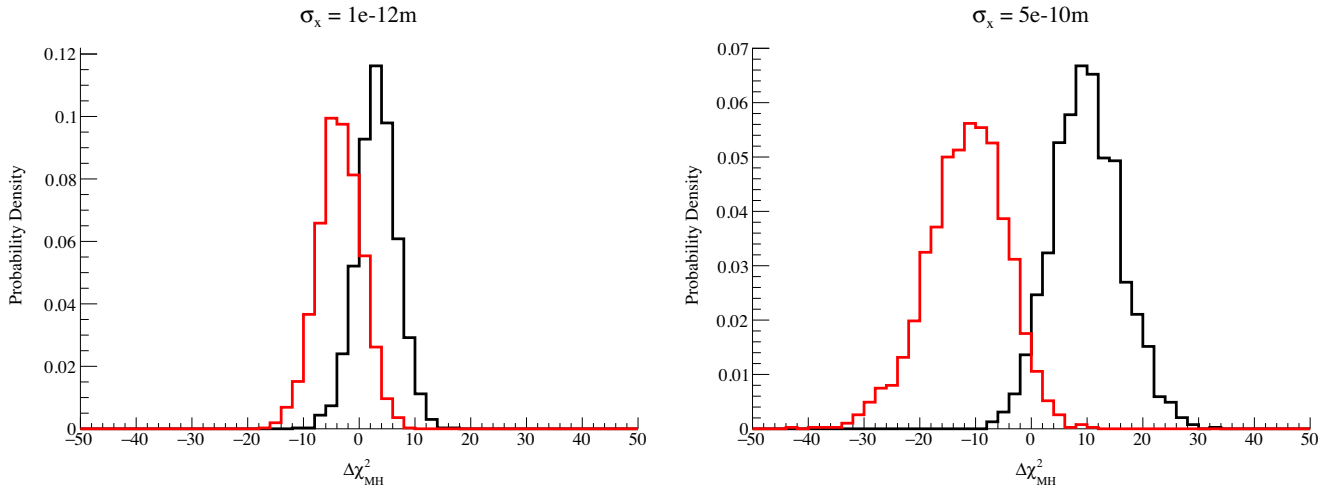

FIG. 2. Distribution of $\Delta\chi^2_{\mathrm{NH}}$ (black) and $\Delta\chi^2_{\mathrm{IH}}$ (red) for two different values of σ_x, 10^{-12} m (left) and 5×10^{-10} m (right). For JUNO, $\sigma_x = 5 \times 10^{-10}$ m is effectively the same as plane-wave oscillations.

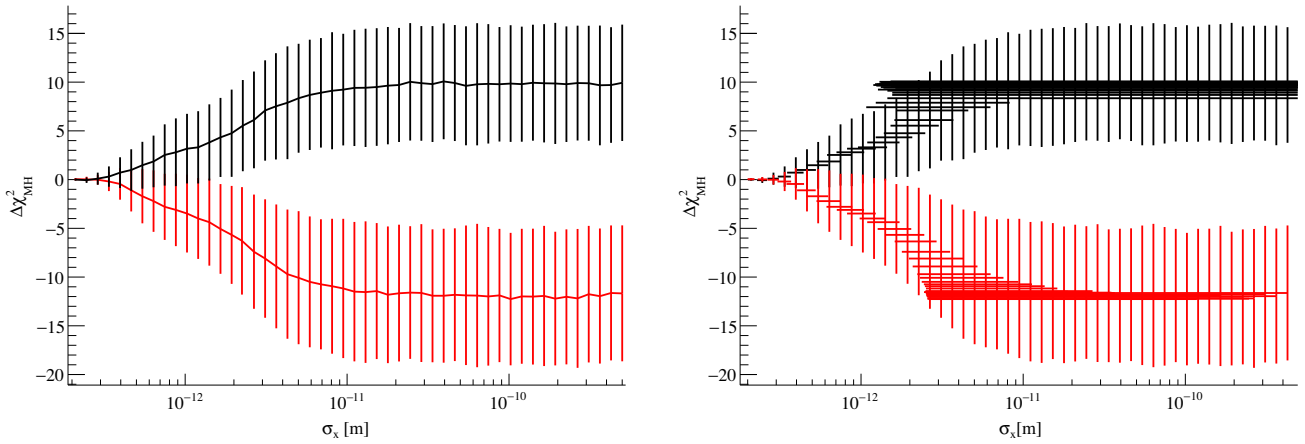

FIG. 3. Left: JUNO's ability to determine the neutrino mass hierarchy as a function of true σ_x for the case of an underlying normal hierarchy (black; $\Delta\chi^2_{\rm NH}$) and an underlying inverted hierarchy (red; $\Delta\chi^2_{\rm IH}$). Right: the same plot, but now showing JUNO's simultaneous ability to measure both σ_x and determine the hierarchy as a function of true σ_x value. For σ_x values above about 4×10^{-12} m, only a lower limit can be obtained. The horizontal error bars represent the bounds of the 68% most central fit results.

hierarchies is significantly degraded in the case of $\sigma_x = 10^{-12}$ m ($|\langle\Delta\chi^2_{\rm NH}\rangle| \sim 3.2$ and $|\langle\Delta\chi^2_{\rm IH}\rangle| \sim 3.4$). In contrast, for $\sigma_x = 5 \times 10^{-10}$ m, the wave-packet effect on oscillation probability is negligible, and therefore consistent with the plane-wave treatment, with $|\langle\Delta\chi^2_{\rm NH}\rangle| \sim 10$ and $|\langle\Delta\chi^2_{\rm IH}\rangle| \sim 12$. The results across a large range of σ_x values are shown in Fig. 3 (left) in terms of both $\Delta\chi^2_{\rm NH}$ and $\Delta\chi^2_{\rm IH}$ as a function of true σ_x. The error bar on each point represents the rms of the distribution of universes while the central value represents the mean. For $\sigma_x > 10^{-11}$ m, the nominal hierarchy determination capability of JUNO is largely unaffected by the finite size of the wave packet. However, the sensitivity to the hierarchy rapidly degrades for $\sigma_x < 10^{-11}$ m, until it disappears around $\sigma_x \sim 10^{-12}$ m.

As might be expected from Fig. 1, there is a range of true σ_x values for which JUNO is sensitive to both σ_x and the orientation of the hierarchy at the same time. Below this range, JUNO is only sensitive to σ_x, and above this range, JUNO is only sensitive to the hierarchy orientation. Figure 3 (right) again shows the behavior of $\Delta\chi^2_{\rm NH}$ and $\Delta\chi^2_{\rm IH}$ as a function of true σ_x, but with the σ_x measurement resolution achievable displayed as well. JUNO can produce a two-sided constraint on σ_x for $\sigma_x < 3 \times 10^{-12}$ m. This result is reasonably consistent with Refs. [12,13]. Figure 4 shows the probability that JUNO will be able to resolve the neutrino mass hierarchy with 95% confidence at different σ_x values for the cases of a true and inverted hierarchy. As can be seen, wave-packet effects detract from JUNO's hierarchy determination capability as far as nearly two orders of magnitude above the current experimental lower limit, up to about $\sigma_x = 10^{-11}$ m. Figure 5 shows the 1σ confidence interval on σ_x that JUNO is likely to produce at different σ_x values. At $\sigma_x = 5 \times 10^{-13}$ m, for example, the expected achievable measurement resolution is $\delta(\sigma_x) = 1.7 \times 10^{-13}$ m. These figures show that for σ_x values between 1×10^{-12} m and 3×10^{-12} m JUNO will likely be able to resolve the neutrino mass hierarchy at 95% confidence and produce a measurement of σ_x.

While sensitivity to the hierarchy can be reduced by finite σ_x, JUNO's expected leading measurements of both $\sin^2\theta_{12}$ and Δm^2_{21}, represented by the depth and energy of the IBD event rate dip around $E_{\bar{\nu}_e} = 3$ MeV in Fig. 1, respectively, are not significantly changed for any experimentally allowed value of the parameter ($\sigma_x > 2 \times 10^{-13}$ m) [8] since, as previously discussed [see Eq. (1)], the slower, solar oscillations, with frequency governed by Δm^2_{21}, are less affected by σ_x.

Similar to Δm^2_{3l}, a measurement of θ_{13} in JUNO, represented by the amplitude of the small, atmospheric oscillations in Fig. 1, would be severely affected by σ_x. Fortunately, θ_{13} has been precisely reported by the Daya

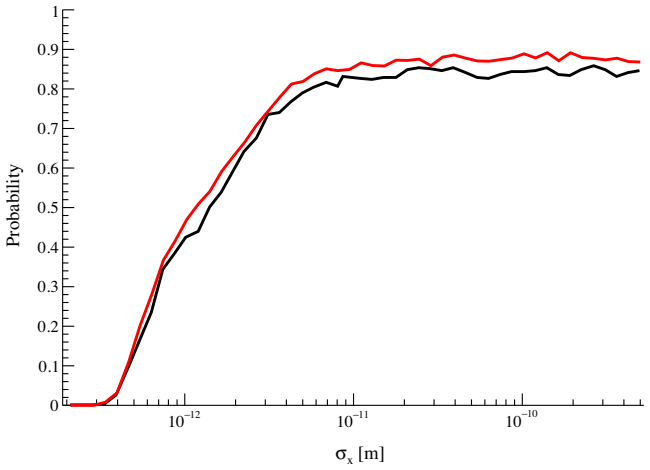

FIG. 4. The probability that JUNO will reject the incorrect hierarchy with at least 95% confidence as a function of σ_x for a true normal hierarchy (black) and a true inverted hierarchy (red).

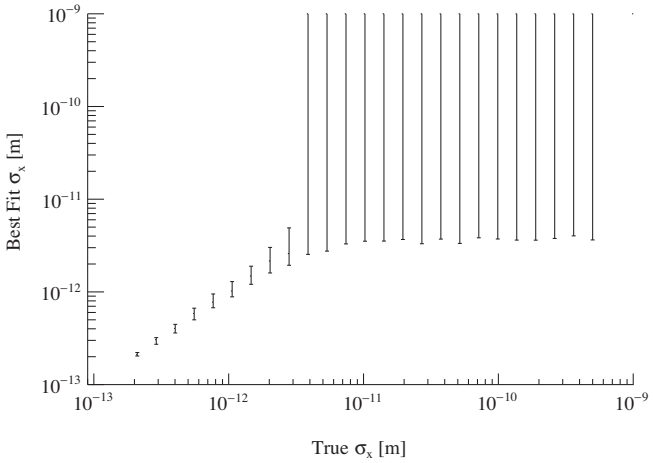

FIG. 5. The 1σ measurement interval JUNO will be able to place on σ_x as a function of true σ_x. For the points with error bars extending above $\sigma_x = 1 \times 10^{-9}$ m, an achievable lower limit measurement is depicted.

Bay experiment [25] and, since JUNO cannot expect to improve upon this measurement, even in the absence of wave-packet effects [10,11], it will rely on this external result. Notably, however, JUNO's sensitivity to both σ_x and the hierarchy, considered individually or together, can be greatly improved with additional, future constraints on Δm^2_{3l} from long-baseline accelerator and atmospheric experiments [26–31]. These experiments, which primarily rely on pion decay-in-flight neutrinos traveling 100s–10000s of km, are insensitive to the wave-packet effect, in the sense that it will not alter their oscillation parameter measurements [7]. Figure 6 again shows $\Delta\chi^2_{\mathrm{NH}}$ and $\Delta\chi^2_{\mathrm{IH}}$ as a function of true σ_x, but with a 50% reduction in the uncertainty on Δm^2_{3l} compared to the current value(s)

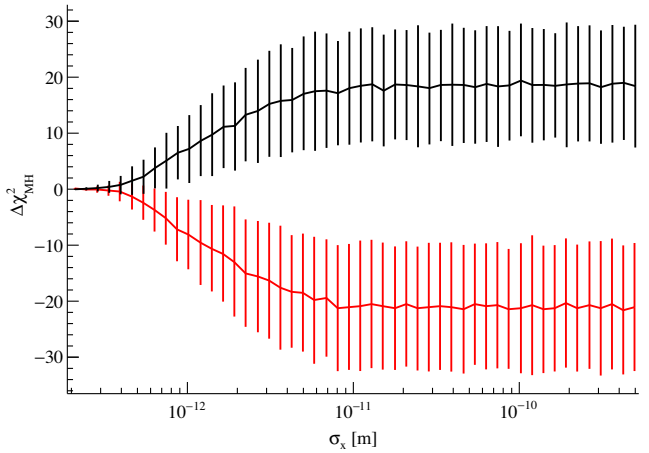

FIG. 6. In the case that the worldwide precision on Δm^2_{3l} improves by a factor of 2 [$\delta(\Delta m^2_{3l}) = (0.028 \to 0.014) \times 10^{-3}\,\mathrm{eV}^2$], JUNO's ability to determine the hierarchy as a function of true σ_x value, for both the case of an underlying normal hierarchy (black) and an underlying inverted hierarchy (red).

shown in Table I [$\delta(\Delta m^2_{3l}) = (0.028 \to 0.014) \times 10^{-3}\,\mathrm{eV}^2$], consistent with projections from a low-exposure DUNE measurement (300 kton · MW · yr) [28], at least, but also roughly representative of expected near-term global improvements informed by T2K [26], NOvA [27], and IceCube [31].

Of course, almost any new neutrino physics relevant at these baselines and energies, such as (e.g.) nonstandard neutrino interactions, neutrino decay, and/or oscillations involving a sterile flavor, seriously encumbers the use of long-baseline $\nu_\mu \to \nu_\mu$ and $\nu_\mu \to \nu_e$ results as inputs for performing medium-baseline reactor-based measurements of $\bar{\nu}_e \to \bar{\nu}_e$. Indeed, any deviation to the three-neutrino paradigm, or standard neutrino interaction paradigm insofar as it is used to extract oscillation measurements, will lead us to revisit many existing results and future sensitivities. While a σ_x measurement and/or hierarchy determination may be confused in such a situation, JUNO's plethora of high-precision results will certainly form an essential global input for either probing this new physics or overly constraining the three-neutrino oscillation paradigm.

Aside from improved external measurements of Δm^2_{3l} (and/or the orientation of the hierarchy itself), realistic future sensitivity enhancements to JUNO in terms of σ_x, the hierarchy, or σ_x and the hierarchy considered simultaneously, other than "more data" given the statistics-limited measurement, are somewhat difficult to envision. One could perhaps consider a smaller spread in reactor baselines, far-detector upgrades, and/or a reliable theoretical prediction for σ_x, as potential sources of sensitivity improvements. The spread in source-to-detector distances leads to oscillated spectrum smearing, with the largest bin migration coming from the currently operating 17.4-GWth Daya Bay reactor complex at 215 km (6.4% of the expected IBD events [11]). Although it is hard to imagine that this complex stops producing power for any significant length of time, which would enhance JUNO's sensitivity, perhaps the JUNO experiment will start taking data before the other long(er)-baseline complex at Huizhou (17.4 GWth at 265 km) comes online in 2025. Improvements to the JUNO energy resolution, primarily driven by photon statistics, would strengthen sensitivity, but JUNO is already at the cutting edge of what is possible with a multi-kiloton-scale detector (77.9% photocoverage, with 17612 20" PMTs @ 34% quantum efficiency [10,11]). A reliable theoretical prediction for σ_x could also offer improved experimental sensitivity to the value and the orientation of the hierarchy, but only in and near the "transition region" presented above ($\sim 10^{-12} < \sigma_x < 10^{-11}$ m), in which the experiment has some sensitivity to both. Even in the case that σ_x is perfectly predicted, sensitivity to the hierarchy cannot be achieved by JUNO significantly below this range.

In terms of JUNO "upgrades" towards improved sensitivity, it is worth emphasizing the need for a near

detector, which is assumed for this analysis, especially in consideration of the possible reactor flux substructure and uncertainties associated with the $5 < E_{\bar{\nu}_e} < 7$ MeV "reactor bump" [14,16,32–35]. Measurements from the near-detector JUNO-TAO (2.8 tons, 30 m from a 4.6-GWth reactor core of the Taishan Nuclear Power Plant; 2000 IBD events per day; sub-1% energy resolution) are expected to constrain the reactor flux bin-to-bin shape uncertainties at the sub-1% level and thereby improve hierarchy sensitivity by $\Delta\chi^2 \sim 1.5$ compared to without [21]. In the absence of this near detector, the reactor flux shape uncertainties are expected at the 2% bin-to-bin level using the Daya Bay reference spectrum, noting Daya Bay's energy resolution of $0.08/\sqrt{E_{\rm vis}(\rm MeV)}$ [21]. However, even with a precision near detector (proximal to a *single* core), uncertainties in the bin-to-bin migration due to the different fission fractions among the many contributing reactor cores, and associated time dependence of these fractions, may be significant. Indeed, reactor flux predictions and their uncertainties are still evolving substantially in time (for a recent example, see Ref. [36]), with the reliant relevant oscillation parameter sensitivities and measurements, including in short- and medium-baseline experiments, following suit (see, e.g., Refs. [37,38]). In general, these issues point to the continued need for theoretical and experimental work towards understanding reactor antineutrino production.

IV. CONCLUSION

We have presented the JUNO sensitivity to both the orientation of the neutrino mass hierarchy in the presence of wave-packet effects and the size of the wave packet itself. We find that wave-packet effects will detract from the hierarchy determination up to nearly two orders of magnitude above the current experimental lower limit, and that JUNO will be highly capable of precisely measuring the size of the wave packet in large regions of currently allowed parameter space. In addition, external experimental measurements, in particular from long-baseline oscillations, will significantly enhance these physics capabilities of JUNO. Given the demonstrated importance of this nonexotic, "standard" quantum-mechanics effect on JUNO, and the experiment's expected contributions to the worldwide neutrino oscillation program, without even mentioning the relevance of the hierarchy determination to cosmological- and terrestrial-based probes of neutrino mass, we would like to encourage more study of the electron antineutrino wave packet, in particular towards forming a reliable theoretical prediction of its characteristic size at creation inside a nuclear reactor.

ACKNOWLEDGMENTS

We thank C. A. Argüelles and B. J. P. Jones for useful discussions. We gratefully acknowledge support from the Department of Energy, Office of Science, under Award No. DE-SC0007859 and the Heising-Simons Foundation.

[1] K. Kiers, S. Nussinov, and N. Weiss, Phys. Rev. D **53**, 537 (1996).
[2] B. Kayser, Phys. Rev. D **24**, 110 (1981).
[3] C. Giunti and C. W. Kim, Phys. Rev. D **58**, 017301 (1998).
[4] C. Giunti, Found. Phys. Lett. **17**, 103 (2004).
[5] N. E. Mavromatos, A. Meregaglia, A. Rubbia, A. S. Sakharov, and S. Sarkar, Phys. Rev. D **77**, 053014 (2008).
[6] P. Huber, Phys. Rev. C **84**, 024617 (2011); **85**, 029901(E) (2012).
[7] B. J. P. Jones, Phys. Rev. D **91**, 053002 (2015).
[8] A. de Gouvêa, V. De Romeri, and C. A. Ternes, J. High Energy Phys. 06 (2021) 042.
[9] F. P. An *et al.* (Daya Bay Collaboration), Eur. Phys. J. C **77**, 606 (2017).
[10] F. An *et al.* (JUNO Collaboration), J. Phys. G **43**, 030401 (2016).
[11] A. Abusleme *et al.* (JUNO Collaboration), arXiv:2204.13249.
[12] A. de Gouvea, V. de Romeri, and C. A. Ternes, J. High Energy Phys. 08 (2020) 018.
[13] J. Wang *et al.* (JUNO Collaboration), J. High Energy Phys. 06 (2022) 062.
[14] F. P. An *et al.* (Daya Bay Collaboration), Phys. Rev. Lett. **116**, 061801 (2016).
[15] S. Abe *et al.* (KamLAND Collaboration), Phys. Rev. Lett. **100**, 221803 (2008).
[16] J. H. Choi, W. Q. Choi, Y. Choi, H. I. Jang, J. S. Jang, E. J. Jeon *et al.* (RENO Collaboration), Phys. Rev. Lett. **116**, 211801 (2016).
[17] C. A. Argüelles, T. Bertólez-Martínez, and J. Salvado, arXiv:2201.05108.
[18] We adopt the NuFIT notation here: $l = 1$ corresponds to $\Delta m^2_{3l} > 0$ (normal hierarchy) and $l = 2$ corresponds to $\Delta m^2_{3l} < 0$ (inverted hierarchy).
[19] Y.-L. Chan, M. C. Chu, K. M. Tsui, C. F. Wong, and J. Xu, Eur. Phys. J. C **76**, 310 (2016).
[20] P. Vogel and J. Engel, Phys. Rev. D **39**, 3378 (1989).
[21] A. Abusleme *et al.* (JUNO Collaboration), arXiv:2005.08745.
[22] I. Esteban, M. C. Gonzalez-Garcia, M. Maltoni, T. Schwetz, and A. Zhou, J. High Energy Phys. 09 (2020) 178.
[23] P. Vogel and J. F. Beacom, Phys. Rev. D **60**, 053003 (1999).
[24] D. Adey *et al.* (Daya Bay Collaboration), Nucl. Instrum. Methods Phys. Res., Sect. A **940**, 230 (2019).
[25] D. Adey *et al.* (Daya Bay Collaboration), Phys. Rev. Lett. **121**, 241805 (2018).

[26] K. Abe *et al.* (T2K Collaboration), Nucl. Instrum. Methods Phys. Res., Sect. A **659**, 106 (2011).
[27] M. A. Acero *et al.* (NOvA Collaboration), Phys. Rev. D **106**, 032004 (2022).
[28] B. Abi *et al.* (DUNE Collaboration), Eur. Phys. J. C **80**, 978 (2020).
[29] M. Jiang *et al.* (Super-Kamiokande Collaboration), Prog. Theor. Exp. Phys. **2019**, 053F01 (2019).
[30] K. Abe *et al.* (Hyper-Kamiokande Collaboration), arXiv: 1805.04163.
[31] M. G. Aartsen *et al.* (IceCube Collaboration), J. Instrum. **12**, P03012 (2017).
[32] J. Ashenfelter *et al.* (PROSPECT Collaboration), Phys. Rev. Lett. **122**, 251801 (2019).
[33] H. Almazán, L. Bernard, A. Blanchet, A. Bonhomme, C. Buck, P. del Amo Sanchez *et al.* (STEREO Collaboration), Phys. Rev. D **102**, 052002 (2020).
[34] Y. J. Ko, B. R. Kim, J. Y. Kim, B. Y. Han, C. H. Jang, E. J. Jeon *et al.* (NEOS Collaboration), Phys. Rev. Lett. **118**, 121802 (2017).
[35] Y. Abe *et al.* (Double Chooz Collaboration), J. High Energy Phys. 01 (2016) 163.
[36] V. Kopeikin, M. Skorokhvatov, and O. Titov, Phys. Rev. D **104**, L071301 (2021).
[37] J. M. Berryman and P. Huber, J. High Energy Phys. 01 (2021) 167.
[38] C. Giunti, Y. F. Li, C. A. Ternes, and Z. Xin, Phys. Lett. B **829**, 137054 (2022).